Article

Reliability analysis and uncertainty evaluation for assessing low velocity car impacted cosmetic damage of prototyped RC bridge pier

Suman Roy

Department of Civil and Environmental Engineering, Utah State University, Logan, UT 84322, USA; sumanroy74@gmail.com

Abstract: Crashworthiness of low velocity vehicles with reinforced concrete (RC) bridge pier has become widespread scenario that warrants a continuous threat on the structural viability. Even, low velocity small car collisions creates a short duration quasi-static to dynamic effect in different damage levels from low and cosmetic to collapse, depending on energy dissipation, not generally considered in design practices, making the piers susceptible to various level of damage. Bridge piers do not always collapse upon impact, and some are kept in service without pertinent health examinations that warrant serviceability. Unfortunately, little attention has been provided to keep the post impact low to medium distressed piers in service. Medium to higher damage need a complete replacement, whereas the low to cosmetic damage needs an additional meticulous investigation. This study is an attempt to assess cosmetic damage and residual capacities of RC pier via pendulum impacts to replicate low velocity car crash scenarios. To investigate post impact performance, experimental results are captured and transformed into realistic crash scenarios. Deterministic analysis via dynamic increase factor (DIF) approach to evaluate damage index (λ) and probabilistic method via resistance reduction method (RRM) to capture the uncertainties are performed in determining residual and reduced capacity of the representative pier. To identify damage incurred from collision and identify the probability of failure (P_f), a limit state (LS) equation has been developed comprising impact load and resistance and utilized as a model to estimate reliability index (β). Both the models used are able to precisely capture reduced capacities providing a good agreement between the shear and the axial capacity which control primary resistance of the impact loads and principal serviceability respectively. This study will provide an aid to forensic structural engineers.

Keywords: low velocity car crash; determination of λ; RRM to determine post impact reduced capacities; a new factor to correlate probabilistic and deterministic approaches; and percent damage

1. Introduction

Crashworthiness of half-sized and prototyped RC bridge piers with low velocity car crash have led a significant influence on the safety, serviceability, and resilience of infrastructural integrity. However, research indicates that the collisions between vehicles and traditional RC bridge piers are the second leading cause of structural bridge failures in the United States [1,2]. Low velocity vehicle impact may cause low to cosmetic damage to the bridge supporting structure which cannot be identified externally by eye estimation. The damage ranges from trivial such as localized cracking of the concrete till spalling cracks and pier fracture, depending on the severity of damage. Bridge piers are often kept into service without adequate investigating the damage level. This low to moderately damaged pier has high possibility to be impacted by the further high strain rate loading caused by nature and humans as well. These include seismic events in the high earthquake prone zones and blast as well due to

various reasons. The dynamic impact load incurred by car crash are not generally considered in design practices, triggering the piers susceptible to extensive damage upon a second impact. In such circumstances, it seems very difficult to predict the post impact performance level followed by damage of the RC pier experiencing respective impacts. Variations in the possible extent of damage to be precisely identified, an in-depth analysis of the pier after impact to certify it for continued service is necessary by having a procedure to accurately determine reduced capacities. Collision analyses of the distressed pier to scrutinize reduced strength has been normally undertaken via static analysis [3]. However, dynamic load incurred from low to moderate velocity impact produces a quasi-static loading that warrants the traditional RC pier from furthering the service and by controlling the post impact pier performance. This study has shed a light on understanding the behavior of material properties of pier under at lower impact investigating the damage level and estimation of the shear capacity [4] and [5]. Characterization of the damage incurred during impact has been estimated via damage index [6]. Unfortunately, inadequate attention has been given to estimating the lesser damage, capturing P_f due to lower impact, and identifying an optimized technique to improve the post impact performance of the piers under combined horizontal impact causing shear and axial compression due to sustained load [7,8].

Studies to categorize the service state of defaced piers from slightly to highly damage have been undertaken according to the intensity and performance level of impact [7]. With regards to high strain rate impact loading experienced by RC bridge piers, the majority of the existing literature focuses on identifying damage levels or increasing survivability [8]. Some research has been carried out for different parameters involved in bridge pier reliability under dynamic loading [9]. Parameters controlling performance of bridge pier under dynamic impact load are primarily controlled by the effects of pier geometry, impact speed and various weights of colliding object, concrete compressive strength, and tensile strength of the reinforcing steel [10]. As the deterministic studies do not precisely capture the risk and uncertainties involved in assessing impact behavior at high strain rate loading, there is a need for probabilistic analysis to ensure exact damage level. Traditional design approach of these structures is often utilized in the most cases, while conservative approach via reliability analysis can only effectively apprehend the low to cosmetic impacted damage, ascertaining probability of failure and corresponding residual capacity.

To economize the design approach, low velocity car impacted loads are usually and unrealistically small [11,12]. However, to achieve a realistic design approach for an RC pier undergoing impact from multiple external agencies and natural calamities, rigorous experimental studies need to be carried out. Investigations comprising various aspects have already been conducted to determine the reliability analysis via resistance reduction method via conducting reliability analysis. As low velocity car impact damage is relatively unknown, this warrants the in-service bridge piers by its reduced strength. In this context, the experimental study is an essential accomplishment to be carried out to scrutinize the post impact performance, behavior, and establish an explicit procedure to accurately determine the residual strength of the in-service RC pier. In this context, to identify damage incurred from car crash scenarios replicated precisely from experimental impact, a limit state model (LSM) equation has been

developed comprising impact load and resistance and utilized as a model to assess P_f and corresponding λ. Results from the experimental studies are captured and have been utilized to establish a prolific post impact performance level corresponding to the reduced capacity of prototyped and half-sized RC piers via various models. To capture the uncertainty for detecting a lower damage level, Monte Carlo (MC) simulations are extensively carried out by determining the P_f and β [13]. This study has been carried out to precisely assess the low impact damage resulting the P_f for smaller vehicle weights and travel speeds to determine respective residual capacities and capture uncertainties involved in experiments. The research undertaken will also help persuading forensic structural engineers in scrutinizing the serviceability of the distressed RC bridge pier, accurately assessing post-performance, and figure out the conclusive health improvement techniques.

2. Test RC pier specimens

To analyze and determine the post impacted reduced capacity of the prototyped pier RC pier specimens in the test program, circular cross-section of two similar piers are considered. The specifications for the representative pier specimens are contemplated from the standardized state department of transportation detail as considered [14]. The pier is assumed to have a uniform circular cross-section with 20 inches' (50.80 cm) gross diameter over its entire length. The unsupported length of the specimens are taken as 6.0 feet (1.83 m). Concrete cover of 1.5 inches (3.81 cm) has been provided for the pier as per the standard specification. End conditions of the specimen is considered as both ends (pier top and bottom) are fixed restraining from rotation and displacement in any direction as shown in **Figure 1a,b**. Schematic diagram including boundary conditions, cross-section considered, and geometries utilized for the pier specimens are as shown in **Figure 1c**.
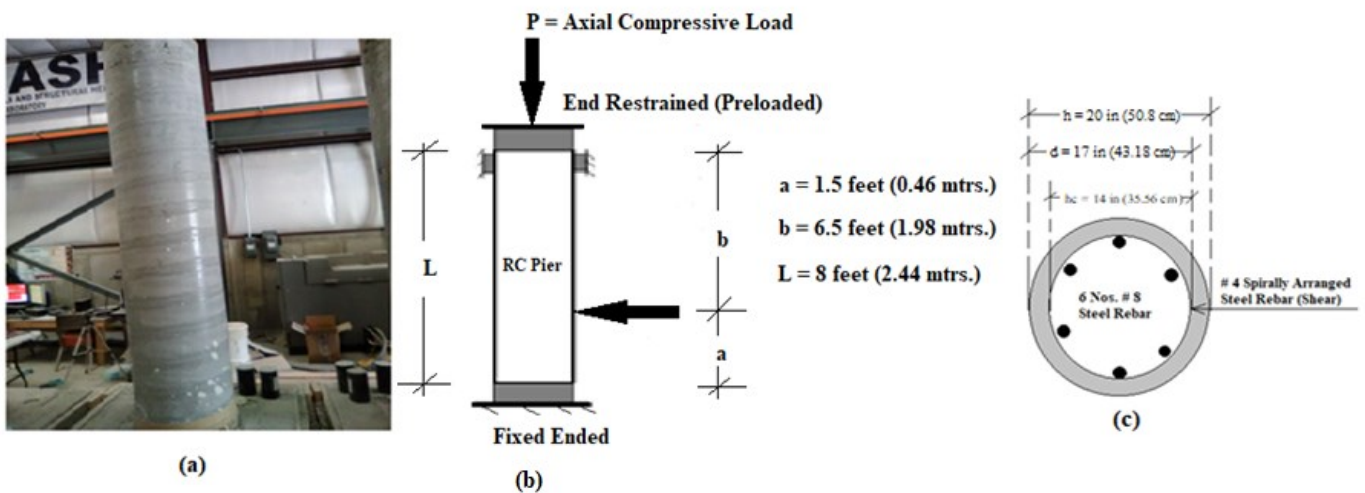

Figure 1. (a) RC pier specimen; **(b)** load and end conditions; **(c)** pier cross-section.

Reinforcement details of test pier specimen

Two numbers cast-in-place traditional RCC circular pier specimens are constructed. Specimens are half-sized with comprising of the main steel reinforcement (primary) of grade 60, i.e., 60 ksi (413.685 MPa) of tensile yield strength are considered from the published data [1], and shear reinforcement (transverse) of grade 36 steel reinforcement (36 ksi or 248.21 MPa tensile yield strength) [15]. Details of the sectional elevation of the RCC pier specimen is as shown in **Figure 2**. The reinforcing details are as shown in **Figure 2** and has been maintained for all test pier specimens. In addition, uniform pier cross-section (20 in. or 50.8 cm diameter) throughout its length is as shown in **Figure 3**.
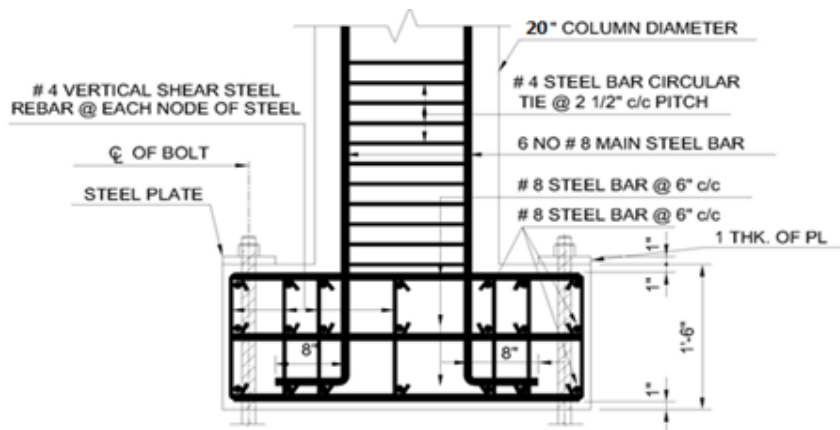

Figure 2. Reinforcement detailing of pier specimen with foundation detailing.

Main reinforcement consists of 6 numbers # 8 steel bars and continues through the foundation bottom. The pier specimen has been designed in a little conservative way to withstand short duration shock resulting the longitudinal steel ratio (ρ_l) of 1.5%. Pier reinforcement is further followed by a spirally arranged shear reinforcement using # 4 steel bar with a transverse steel ratio (ρ_t) of 0.06% conforming minimum reinforcement criteria. Vertical pitch for shear reinforcement is utilized at 2.5 inches (63.5 mm) throughout the test specimen. Shear reinforcement provided in the specimens conforming the minimum shear reinforcement criteria [16–18]. In addition, the representative test pier specimen also satisfies the shear reinforcement criteria for reinforcing bar diameter utilized for flexure (longitudinal), shear (lateral) and pitch of the lateral reinforcement [19]. The details of the test pier specimen are shown in **Table 1**. Specimens with same geometries and materials are constructed to carry out the tests.

Table 1. Details of specimens.

h (in) (cm)	A_g (in²) (cm²)	A_{st} (in²) (cm²)	A_{net} (in²) (cm²)	ρ_l (%)	ρ_t (%)	f'_c (ksi) (MPa)	f_y (ksi) (MPa)
20 (50.80)	314.28 (2027.60)	4.74 (30.58)	309.54 (1997.02)	1.5	0.06	7.00 (48.26)	60 (413.68)

In **Table 1**, h, A_g, A_{st}, A_{net}, present the diameter of pier, gross cross-sectional area of pier, area of main reinforcing steel rebar used in pier section and net cross-sectional area of the pier. Compressive strength of concrete and yield strength of steel are represented as f'_c and f_y respectively. In addition, ρ_l and ρ_t are representing steel ratios

used as longitudinal and transverse reinforcement respectively as shown in **Table 1**.

Ready mix concrete (RMC) has been used to pour down concrete in order for making cast-in-place RC pier specimens including foundations. Sono-tubes are utilized as column shuttering. The pouring was made in two stages for column casting. Maximum size of the coarse aggregate used was ¾ inches (20 mm down) in concrete mix. The concrete mix has been prepared by using medium to fine aggregates and normal weight Portland cement available in the market. The reinforcement pier-foundation detailing as stated in **Table 1** is further furnished at **Figure 2**.

3. Determination of vehicular impact

Test specimens are designed conforming specification in such a way to withstand dynamic load conditions [16,17]. Specimens' designs are also checked for confirming axial, shear, bond, with the equivalent static of dynamic loads. A little consideration is given by providing adequate lap and development length of reinforcing steel bars. However, dynamic effects incurred by impact and shock play a major role to control post impact behavior. To evaluate the effects of impact loads on RC piers, the dynamic impact force is estimated as an equivalent static force as described in this section.

3.1. Dynamic force due to vehicular impact

Assuming the vehicle comes to rest without rebounding from pier specimen, the kinetic energy (E) equations can be determined by using Equation (1) [18].

$$E = 0.5 M_{veh} V^2 \qquad (1)$$

where: M_{veh} indicates the classification of weight [5] as shown in **Table 1**, E and V represent the impact energy and vehicle frontal impact velocity respectively.

The equivalent vehicular velocities of impact (V) determined considering approximately 72% energy dissipation and is as shown in the Equation (2) [19].

$$V = 2.67 \sqrt{\left(\frac{W}{M}\right) \times (gH)} \qquad (2)$$

where: W, M, g, and H represent pendulum weight, weight of the impacting vehicle, acceleration due to gravity at specific altitude, and height of fall for impact.

Table 2. Equivalent car impacting velocities [20].

Car Type	Picture	M_{veh} in lbs. (kN)	V in feet/sec (km/hr)
Sub-Compact Car		2505 (11.14)	33.54 (36.80)
Mid-size sedan Car		3361 (14.95)	32.83 (36.02)

The equivalent car (Class-I) impact results replicated from the pendulum impact tests and the corresponding results are utilized to determine low velocity impacts using Equations (1)–(4) as shown in **Table 2**.

The dynamic impact force (I_{dyn}) exerted by the small car for low velocity impact (as shown in **Table 2**) on the pier specimen is represented using the pressure criteria

induced and transmitted from the impacting vehicle. Its geometric dimensions and the duration of impact are also shown in Equations (3)–(5) as described in [21,22]. Time of short-duration impact is characterized using as half sine function comprising amplitude as the peak impact force (PIF). The function is considered representing the shock pulse as it is intrinsic characteristic of the post impact phenomena over its duration. An averaged integration is then used to determine the equivalent static force incurred from the impact pulse. The averaged integration is executed over a small window around the PIF to obtain a conservative estimate that accurately reflects the load transferred to the pier from the vehicle during the peak of the impact. The PIF is conservatively determined as a function of the kinetic energy (E) transmitted to the pier from the colliding car, the geometric dimensions of specimen, material properties utilized to build specimens, and the impact duration (t) are respectively shown respectively in the Equations (3)–(5) as stated by [23,24].

$$I_r = \{(2 \times 10^{-5} E_{eff}) + 386.48\} \left[\frac{(I \times L)}{(a \times b \times c)} \right] \tag{3}$$

$$t = \sqrt{\frac{M}{k}} \tag{4}$$

$$I_{dyn} = \frac{\int_{t_d - 0.025}^{t_d + 0.025} I_r \sin\left(\frac{\pi t_d^+}{t}\right) di}{0.05} \tag{5}$$

where: I_{dyn} represents the frontal shock (force) due to impact, I_r is the peak reflected pressure (overpressure), t_d^+ is the time instant of the peak impact force, t represents the impact duration, E is the kinetic energy absorbed by the impacted bridge pier. As shown in **Figure 3**, L is the unsupported length of the pier, a is the distance from the bottom of the pier to the point of impact, b is the distance from the top of the pier to the point of impact, and c is the perpendicular distance from the neutral axis (NA) of the cross section to the farthest point (extreme fiber) on the cross section of the pier, M is the weight of the impacting vehicle, and k is the vehicle frontal stiffness [12,24].
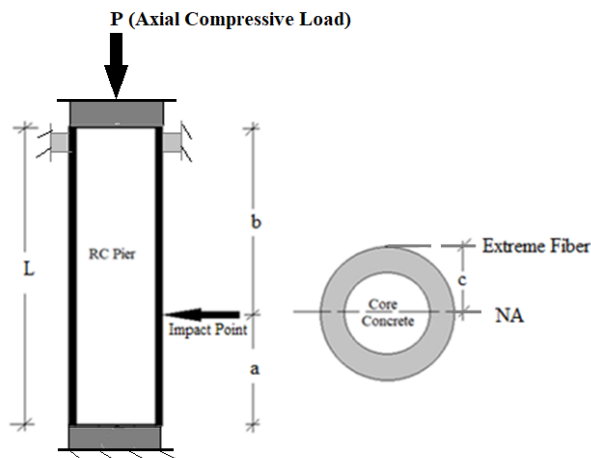

Figure 3. Impact location and geometry of RC bridge pier [24].

3.2. Experiments of pendulum impact

There are two types of impact were taken place. All two specimens of the test

piers were impacted by the push-over in order to generate the seismic event. First, the single test column undergone only push-over whereas the rest four were undergone first by pendulum impact, followed by push-over experiment. Test setup consisting of the colliding pendulum is provided to apply an impact bending load at test pier, schematic diagram has been shown in the **Figure 4**.
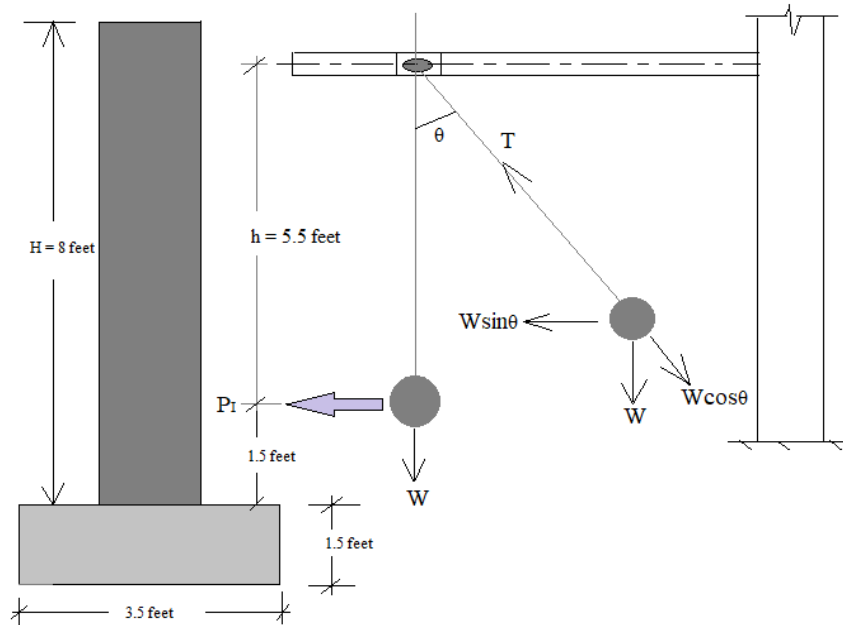

Figure 4. Schematic diagram of pendulum impact.
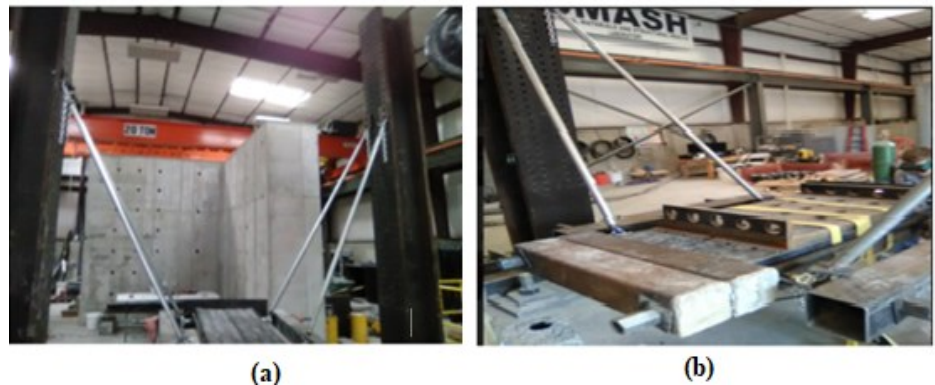
Figure 5. In site built-up pendulums. **(a)** 1.75 kips; and **(b)** 2.25 kips.

This type of low velocity impact will result some damage followed by post impact deformations due to transfer of impact energy into the kinetic energy (E). The 1.75 kips (7.78 kN) and 2.25 kips (10.00 kN) spherical pendulums (as shown in **Figure 5**) have been utilized for impacts which produce approximately effective impact energies respectively after substantial dissipation [25]. This experimental procedure complies with the specifications outlined in the standards, ASTM E23-18 and ISO 148-3:2016 [26]. Pendulums are designed to replicate the same impacts produced by small cars on the prototyped pier specimens as shown in **Table 2** as per the design calculations executed using Equations (1) and (2). The impact effects are estimated to replicate low velocity small car hit on the pier specimens by using Equations (3)–(5).

Determination of static load capacity

To determine the design axial and shear capacities in the representative pier specimens, standard specification of ACI has been utilized [3]. The axial capacity ($P_{N,design}$) of pier specimen is evaluated as shown in Equation (6) [16].

$$P_{N,design} = 0.85 \times f_c' \times (A_g - A_s) + \sigma_y \times A_s \tag{6}$$

where: f_c' is the 28-day compressive strength of concrete, f_y is the yield strength of steel, and A_g and A_{st} are the gross cross-sectional area of concrete and total cross-sectional area of longitudinal steel, respectively. $P_{N,design}$ is computed as 2126.16 kips (11,034.61 kN). The axial load (preloading) applied on each test specimen was initially considered as 80% of the axial capacity and are as shown in **Table 3**. The detailed result of the axial capacity of the RC pier including preloading is as shown in **Table 3**.

Table 3. Design axial capacity of pier specimen.

h (in) (cm)	A_g (in²) (cm²)	A_{st} (in²) (cm2)	*f'*$_c$ (ksi) (MPa)	*f*$_y$ (ksi) (MPa)	$P_{N,design}$ (kips) (kN)	Preloading (kips) (kN)	Percent Preload (Initial)
20 (50.80)	314.28 (2027.60)	4.74 (30.58)	7.00 (48.26)	60 (413.68)	2126.16 (9457.63)	1700.00 (7561.97)	80

The test pier specimens comprising with the design shear capacity is estimated using Equation (7) as specified in AASHTO 2011 [27].

$$V_{N,design} = V_c + V_s \tag{7}$$

where: V_c is the shear strength carried by the concrete and V_s is the transverse shear capacity; V_c (shear strength) is determined via Equation (8) as specified in [27].

$$V_c = v_b[1 + 3P_{N,design}/f_c'A_g]A_e \tag{8}$$

where: A_g represents the gross cross-sectional area of the concrete in the pier and A_e is 80% of A_g, i.e., $A_e = 0.8 \times A_g$, and v_b is the shear constant; v_b (shear constant) is determined using Equation (9) as stated in the specification [27].

$$v_b = [0.0096 + 1.45\rho_t] \times (f_c')^{1/2} \leq 0.03(f_c')^{1/2} ksi \tag{9}$$

where: ρ_t is the longitudinal steel ratio and $P_{N,design}$ represents the axial load capacity of the reinforced concrete pier; V_s (Transversal shear capacity) is estimated using Equation (10) as furnished in AASHTO M145-91 2008 [27,28].

$$V_s = (\pi/2)(A_h\sigma_{yh}) \times (D'/s) \tag{10}$$

where: A_h is the area of a single hoop or spiral, D' is the spiral or hoop diameter, s denotes the pitch of the helix, and σ_{yh} represents the yield stress of transverse reinforcing steel bar.

3.3. Dynamic Impact Factor (DIF)

The dynamic impact factor (DIF) can be defined as dynamic to static load incurred by the member. This can be expressed in terms of quasi-static strain rate ($\dot{\varepsilon}$) of reinforcing steel for tensile strength as shown in Equations (11)–(13) [29].

$$\sigma_{dyn} = [1 + (\dot{\varepsilon}/C)^{1/P}]V(f_y + \beta E_p\varepsilon^{eff}) \tag{11}$$

$$\xi = 0.019 - 0.009 \times \left(\frac{\sigma_{dyn}}{60}\right) \tag{12}$$

$$DIF = \left(\frac{\acute{\varepsilon}}{10^{-4}}\right)^{\xi} \tag{13}$$

where: $\acute{\varepsilon}$ is the strain rate considered as 5.4×10^{-4} s^{-1} [26], ξ is a constant which depends on the dynamic yield stress of steel at the strain hardening zone, parameters C and P indicate the strain rate parameters [30]. σ_{dyn} is the dynamic yield stress of reinforcing steel, f_y is the initial yield stress, which is taken as 60 ksi (420 MPa) as per ASTM A706 for the yield stress at the elastic zone for grade 60 steel bar, ε_{eff} is the equivalent plastic strain, taken as 0.72, E_p is the plastic hardening modulus, β is the hardening parameter which ranges from 0 to 1 and is taken as 0.5 in this study, and

The modulus of elasticity (E_P) of the steel bar at the strain hardening stage can be determined by using Equation (14) [30].

$$E_p = \frac{\sigma_p}{\varepsilon_{eff}} \tag{14}$$

where: σ_P represents the yield stress at plastic region used in the Equation (16) is 8.612 ksi (59.376 MPa) and the plastic strain, ε_{eff}, used is 0.72 as specified in ACI committee 318 1985 [16,17]. The modulus of elasticity, E_P, is determined to be 11.94 ksi (82.32 MPa) [26]. After inserting these values into Equation (13), results in dynamic yield stress (σ_{dyn}) is computed as 68.61 ksi (473.05 MPa).

Using Equation (13) with the calculated dynamic yield stress σ_{dyn} of 68.61 ksi (473.05 MPa), yields ξ as 8.7×10^{-3} using Equation (14), resulting in a DIF of 1.02 according to the Equation (15).

3.4. Computation of damage index

The damage of RC member under impact load can be appraised by using a standardized scale termed as damage index (λ). Computed as a ratio of the equivalent static force from the impact to the shear capacity of the pier with the respective external dynamic force, λ can be determined via Equation (15) [31].

$$\lambda = I_{dyn}/V_{dyn} \tag{15}$$

where: I_{dyn} is the peak vehicle dynamic impacted force, and V_{dyn} indicates the dynamic shear effect on concrete.

The dynamic shear (V_{dyn}) of the pier is a function of the strain rate behavior of the concrete as encapsulated in the DIF. Computed and as shown in Equation (16) [17,24,25], the dynamic shear capacity offers an insight into the expected behavior of concrete under dynamic loading events [31].

$$V_{dyn} = DIF \times V_{N,design} \tag{16}$$

The relationship between the λ and residual strength (L_R) of the damaged pier is shown in Equation (17) [31].

$$L_R = (1 - \lambda) \times L_{Design} = \zeta_D \times L_{Design} \tag{17}$$

where: L_R is the residual strength for axial or shear of the damaged pier after experiencing vehicular impact, L_{Design} is the design axial or shear load carrying capacity of the undamaged RC bridge pier as specified [17], and ζ_D is the factor used for evaluating residual capacity via performing deterministic analysis and shall be obtained from Equation (18).

$$\zeta_D = 1 - \lambda \tag{18}$$

Using the DIF value obtained from Equation (15), the dynamic shear force (V_{dyn})

can be determined for the representative pier by using Equation (18). The V_{dyn} is thus a function of vehicular weights, impacting velocity and impact duration. As such, it is determined that these variables play a significant role in precisely predicting the level of damage subjected to short duration vehicle impact load incurred by RC bridge piers.

4. Determination of post impact damage

In this study, post impact cosmetic damage is evaluated through reliability assessment from determining the probability of failure from the specific load scenario. In the first stage, reduced resistance caused by post impact vehicle damage is determined by resistance reduction method (RRM), via using Monte-Carlo (MC) simulations. Due to uncertainty involved in capturing residual capacities caused by low impact scenarios, deterministic analysis seems a little indecisive in precisely capturing the probability of failure, probabilistic analysis is thus carried out to estimate the post impacted cosmetic damage level.

LSE analytical method

Using Equations (11)–(14), and Equation (16), it can be surmised that the load model is based on the dynamic impact while the resistance model is based on the dynamic shear capacity of the pier. Both these models are comprised of parameters which are random variables. The basic parameters defining a random variable are its mean, standard deviation, and distribution. These encapsulate the uncertainty inherent in design values of these parameters. As such, utilizing the mean and standard deviation in lieu of the nominal design values of the parameters capture the uncertainties in the probabilistic analysis [23].

However, structural serviceability for the limit state function (g_i) comprises with the performance not exceeding permissible function as shown in Equation (19). This shows the limit state equation satisfying the serviceability criteria [23].

$$g_i = 1 - \lambda = 1 - \frac{I_{dyn}}{V_{dyn}} \tag{19}$$

where: g_i is the limit state function, I_{dyn} is the peak vehicle dynamic impacted force, and V_{dyn} indicates the dynamic shear effect on concrete as mentioned in Sec. 3.3.

Nominally, the probability of failure (P_f) is determined by integrating the limit state function over the region where the limit state function is less than or equal to zero as expressed in Equation (20) [32].

$$P_f = \int_{Z=-\infty}^{Z \le 0} f_x(x_1, x_2, \ldots, x_n) \, dx_1 dx_2 \ldots dx_n \tag{20}$$

where: f_x is the joint PDF of the random vector $X = \{X_1, X_2, \ldots, X_n\}$, and $Z = g(x) < 0$; that is the region of failure. This is further illustrated within the region, $-\infty = Z \le 0$, where the failure of RC bridge pier due to vehicle impact is expected to occur.

However, determining the probability of failure by evaluating the integral shown in Equation (16) is quite complex. Alternatively, a reliability index for a structure or structural member can be computed and then used to compute the probability of failure. Converse to the probability of failure, the reliability index (β) is a measure of structural reliability which captures the inherent influence of parameter uncertainties [22]. Accordingly, several methods have been developed for assessing the reliability of structural members and by extension the probability of failure. To capture the

cosmetic damage level at low impact scenario, MC simulations are utilized to capture the corresponding P_f. These methods usually return slight variations in β and P_f. The estimated β in its simplest form is computed using the uncertainty parameters (mean and standard deviation) as shown in Equation (21) [33].

$$\beta = \frac{\mu}{\sigma} \tag{21}$$

where: μ is the mean of the and σ is the standard deviation of the limit state equation (LSE).

However, computing the μ and σ of the LSE is often impractical especially when LS is a nonlinear function. Also, it presents problems in dealing with LSE where the probability distribution is not normal. As a result, an alternate method of computing the β involves using MC simulations. This method involves simulating the LSE a number of times with changing the respective design variables. These design variables are developed using the uncertainty parameters and randomly generated numbers as shown in Equations (22) and (23) [33].

$$x_i = \mu_x + z_i \sigma_x \tag{22}$$
$$z_i = \Phi^{-1}(u_i) \tag{23}$$

where: x_i is the computed variable, z_i is standard normal variable, u_i are uniformly distributed random variables ranging between 0 to 1, and Φ^{-1} is the inverse of the standard normal cumulative distribution function.

The LSE is then solved using the generated variables by using RAND function via EXCEL. This process is repeated many times using randomly generated uniformly distributed variables. The P_f is then estimated by dividing the number of times the LSE simulation is less than 0 by the total number of simulations (N) carried out. The β can be directly computed from the P_f as shown in Equations (24) and (25) [34].

$$P_f = \frac{n}{N} \tag{24}$$
$$\beta = -\Phi^{-1}(P_f) \tag{25}$$

where: n is the number of times the limit state was exceeded ($g(x) < 0$), and N is the total number of simulations undertaken.

A recently developed method to resolve some of the challenges with using the fault tree analysis is the resistance reduction method [33]. This method works to capture the reduction in capacity of a structure due to a loading event by utilizing the probability of failure of the structural member particularly at low impact to apprehend the damage level and determining the corresponding residual capacities. A resistance reduction factor is computed and then used as a multiplication factor to adjust the structural capacity of a member after the loading event. This resistance reduction factor (ζ_P) is computed as the complement of the P_f using probabilistic analysis and is as shown in Equation (26) [25].

$$\zeta_P = 1 - P_f \tag{26}$$

where: ζ_P is the resistance reduction factor and P_f has already been stated.

Similar to the damage index (λ), the RRM can be used to effectively reduce the design capacity to the residual capacity by multiplying the factor by the design capacity, thus accounting for the damage incurred by the pier during the impact event. Reduced capacity of the impacted pier through probabilistic analysis can be obtained from Equation (26).

$$L_{Reduced} = \zeta_P \times L_{Design} \tag{27}$$

where: ζ_P is the resistance reduction factor evaluated via probabilistic approach, L_{Design} is the design capacity, and $L_{Reduced}$ is the reduced capacity of the impacted pier at specific loading event.

The reliability analysis requires design parameters to be treated as random variables and their statistical parameters (mean and standard deviations) as well as their distributions are used in determining the reliability index. **Table 4** outlines the random variables and their distributions. The parameters for the geometric dimensions as well as the material properties are obtained from past studies as published in [35]. The vehicle mass parameters are obtained from weigh in motion data for the state of Utah [36] and the vehicle speed parameters from [25,26]. The pitch of the transverse reinforcement is assumed to remain constant and is not a random variable. Design variables comprising individual uncertainty parameters are given in **Table 4**.

Ten thousand Monte Carlo simulations are carried out for limit state function to determine reduced capacity [37] which is correspondent to the probability of failure. To evaluate this, statistical parameters, mean and standard deviation are utilized to converge at about this number of simulations. Random numbers are generated using 'RAND' function [26]. Design variables and uncertainty parameters used in the simulations are provided in **Table 4**.

Table 4. Design variables and their uncertainty parameters.

No.	Variables	Distribution	Mean	St. Dev.	Units
1	Diameter of pier (h)	Normal	20.00 (0.51)	0.25 (0.006)	inches (m)
2	Height of pier (L)	Normal	100.06 (2.54)	0.25 (0.006)	inches (m)
3	Vehicle weight (M_{veh})	Normal	Varying	-	lbs (kN)
4	Vehicle velocity (V)	Lognormal	Varying	-	ft/s (m/s)
5	Core concrete diameter (d_c)	Normal	17.00 (0.43)	0.25 (0.006)	inches (m)
6	Yield strength of transverse Reinforcement (σ_{yt})	Lognormal	40,770 (280.62)	4729.32 (32.55)	psi (MPa)
7	Compressive strength of concrete (f'_c)	Normal	Varying	-	psi (MPa)
8	Diameter of longitudinal reinforcement (d_l)	Normal	0.855 (0.021)	0.365 (0.009)	inches (m)
9	Yield strength of longitudinal reinforcement (σ_y)	Lognormal	67,500 (465.40)	6615 (45.61)	psi (MPa)
10	Diameter of transverse reinforcement (d_t)	Normal	0.56 (0.014)	0.365 (0.009)	inches (m)
11	Confined hoop diameter	Normal	17.355(0.44)	0.365(0.009)	inches (m)
12	Stiffness (k)	Normal	1,713,045 (300.00)	342,609 (60.00)	lb/in (kN/m)
13	Pitch (s)	Deterministic	2.5 (0.06)	-	inches (m)

5. Results and analysis

5.1. Observations of the specimen failure

Results are shown in this section is primarily based on the observations to detect the cosmetic damage and the corresponding damage collapse as a consequence of pendulum impact test. The post impacted test specimens can apprehend the performance at specific impacts, replicated well from small sized car crashes, and capturing the failure pattern by depicting the corner failure via load transmittance path,

and hence validated the analytical model through recognizing the cracks as shown in **Figure 6**. The cracks developed during the load applications of 1.75 kips and 2.25 kips through built-up pendulum impacts. The pendulum impact processes were designed in such a manner that it can also well capture low velocity car crashes and able to replicate the failure patterns because of similar dissipation path of respective load transmittance via energy dissipation.

However, in addition to the spalling and vertical cracks in the respective test specimens as shown in the **Figure 6**, there could be high possibilities of developing and presence of the internal cracks in the specimens. Those hair can barely be observed and estimated by eye estimation. This leads a higher uncertainty to assess the damage level and needs an in-depth analysis.
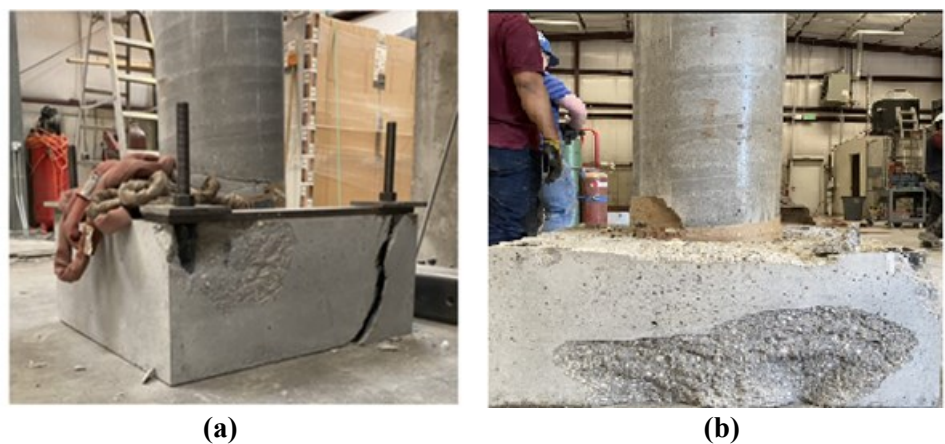

(a)   **(b)**

Figure 6. Post impact damage of **(a)** Pier 1; **(b)** Pier 2.

5.2. Residual capacities through deterministic analysis via damage index (λ) method

Alike the process used in estimating the reduced capacity of a RC pier after impact, the post impact axial and shear capacities of RC piers for different compressive strengths are first determined using deterministic method via damage index (λ), and compared the results evaluated through probabilistic method via utilizing resistance reduction factor. **Table 5** shows the deterministic residual capacities which is further clarified in **Figure 4** apprehending the residual axial and shear capacities for various vehicle weights at specified impacting speeds.

Table 5. Residual capacities using deterministic analysis.

Car Type	M_{veh} (kip) (kN)	V (feet/sec) (m/sec)	$P_{N,residual}$ (kip) (kN)	$V_{N,residual}$ (kip) (kN)
Sub-compact	2.505 (11.14)	33.54 (10.22)	1816.61 (8080.68)	261.19 (1161.83)
Mid-size sedan	3.361 (14.95)	32.83 (10.00)	1641.30 (7300.87)	235.98 (1049.69)

Deterministic analysis via damage index (λ) method to evaluate the low to moderate damage level are utilized to ascertain residual capacities of the impaired pier. This study is conducted to evaluate damage incurred by low impact velocities of the car. Representative prototype RC pier is investigated as a performance against post

vehicle impact behavior in terms of residual axial and shear capacities for specific vehicle weights at specific impacting speeds. The respective performance level of the post impacted RC pier is compared and is shown in **Figure 7**.
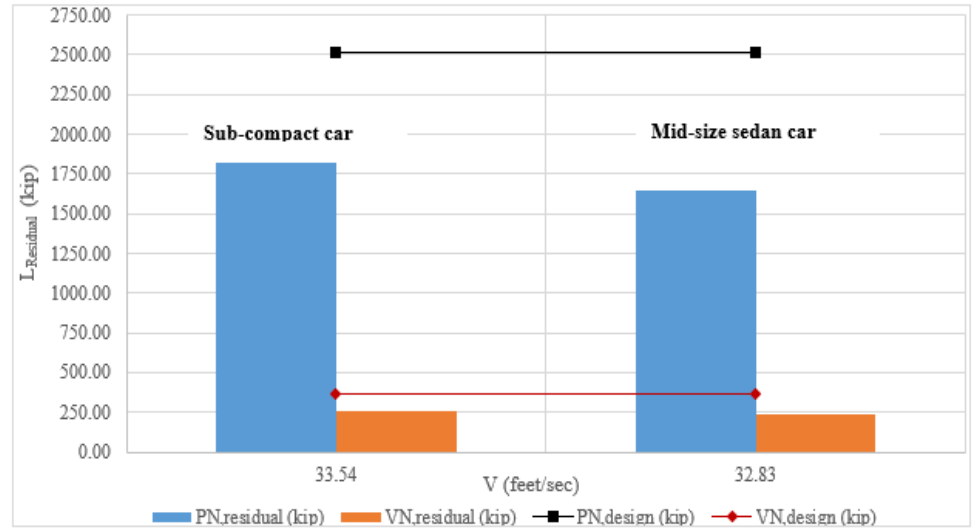

Figure 7. Residual capacities of RC pier impacted at specific vehicle weight at specific impacting speed.

5.3. Reduced capacities through probabilistic analysis via MC simulation

Monte Carlo (MC) simulation is undertaken for the limit state function (g_i) with the inverse of the cumulative distribution function (CDF) for the P_i, i.e., $\Phi^{-1}(P_i)$, subject to the high strain rate loading. The simulations that are conducted are shown in **Figures 8** and **9** respectively. The probability of failure (P_f) and the inverse of the cumulative distribution function (CDF) for the P_i that are plotted using ten thousand MC simulations (statistical parameters mean and standard deviation converged at about this number of simulations).
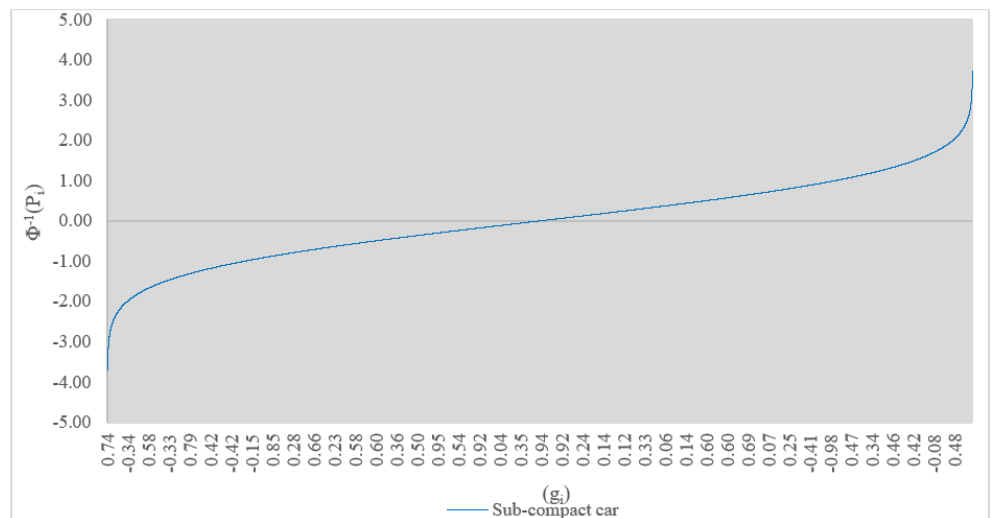

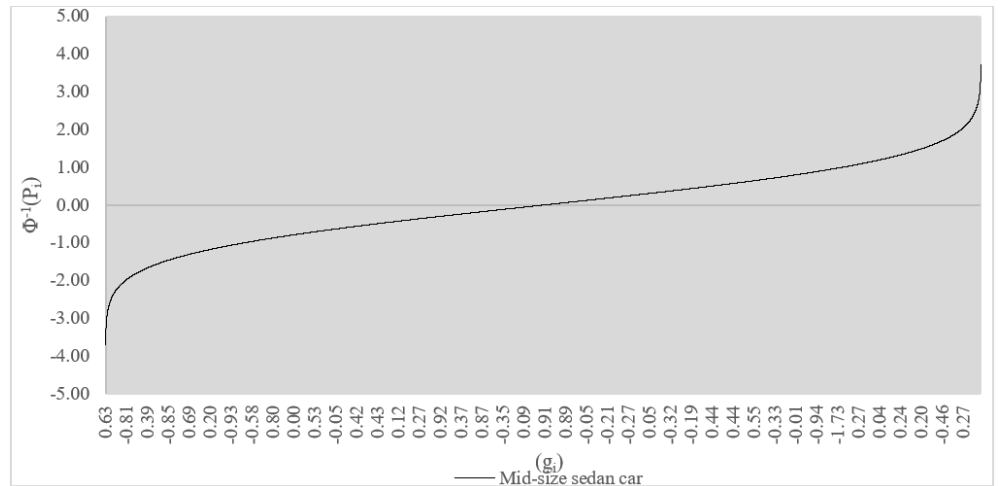**Figure 8.** Monte Carlo simulation for sub-compact car impact.

Figure 9. Monte Carlo simulation for mid-size sedan car impact.

Due to uncertainty involved in capturing residual capacities caused by low impact scenarios, deterministic analysis seems a little indecisive in precisely capturing the P_f, probabilistic analysis is thus carried out to estimate the post impacted cosmetic damage level.

Probability of failures (P_f) determined from **Figures 5** and **6** are 0.21 and 0.39 respectively. Using Equation (25), β can be found as 0.81 and 0.28 respectively. ζ_P values have been evaluated as 0.79 and 0.61 using Equation (26). The corresponding reduced capacities are determined by using Equation (27), and the results are summed up and is shown in **Figure 10**.
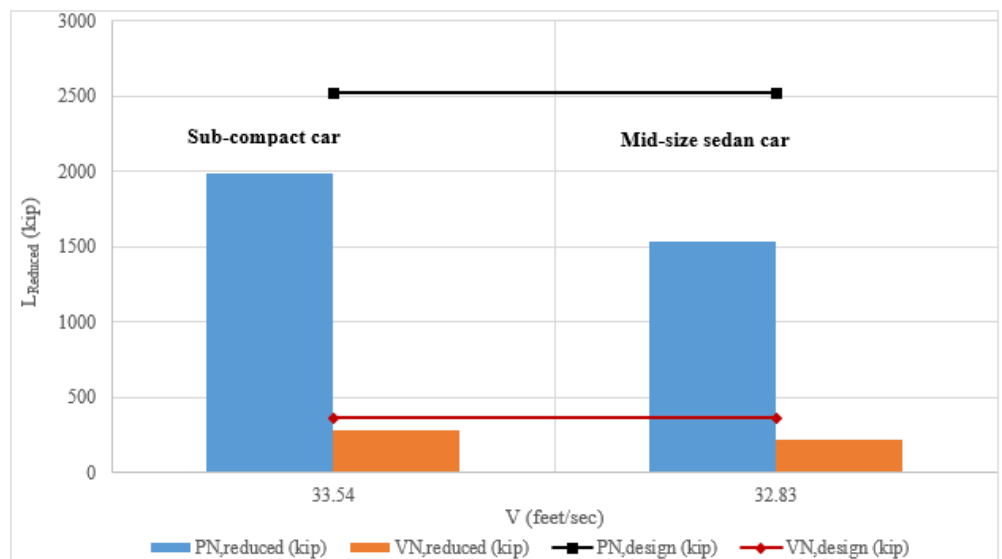
Figure 10. Residual capacities of RC pier impacted at specific vehicle weight at specific impacting speed.

6. Discussion of results

This present study discusses the results extracted from the experimental work which is then transformed into the realistic cosmetic damage scenarios usually not captured by the deterministic analyses [38]. The analytical method which has been developed based on the effects of the DIF to determine L_R of a prototyped pier

specimens subjected to low velocity vehicular impact. Probabilistic analyses utilized to capture uncertainties via incorporating RRM are also performed in determining residual and reduced capacity of the distressed specimens. Two methods utilized in estimating the post impact residual capacities are compared to develop a new safety factor (ψ). The first method, using the λ, involves computing a damage level. This ratio (ζ_D) is subtracted from one and used as a multiplier to reduce the structural capacities of the pier. The second method goes further in utilizing the damage index (DI) equation as an LSE to compute the P_f of the pier at specific impact, and then uses this P_f to compute a ζ_P. The ζ_P is then utilized as a multiplier to reduce the design capacities, thus obtaining the post impacted residual capacities. The RRM was found to be slightly more conservative specifically in determining shear capacity, estimating lesser L_R values at lower speeds than the corresponding higher vehicle weights.

Analyzing results for two different speeds and different vehicle weights allowed for some conclusions to come up with an improved decision. Results plotted in the **Figures 4** and **7** indicate that in order to optimize the axial and shear capacities of an RC pier, deterministic method using damage index approach provides conservative results in evaluating residual capacities from vehicle impact damage incurred by sub-compact car, whereas probabilistic analyses using resistance reduction method provides conservative results for the damage experienced by mid-size sedan car capturing uncertainties involved in estimating low to cosmetic damage. The difference in determining the post damaged capacity estimated by probabilistic method provides 8.68% increase than that of the deterministic analyses for sub-compact collision, whereas it provides a conservative result of 6.86% for being damage incurred by the mid-size sedan car for both axial and shear capacities. The results for deterministic, probabilistic, and percent difference in estimating the residual capacities are shown in **Table 6**.

Table 6. Factors estimating residual capacities.

Car Type	Deterministic		Probabilistic		Percent difference	
	λ	ζ_D	P_f	ζ_P	Axial	Shear
Sub-compact	0.28	0.72	0.21	0.79	8.68	8.68
Mid-size sedan	0.35	0.65	0.39	0.61	6.86	6.86

The results can be put together by introducing a safety factor (ψ) being a ratio of the two factors used to determine post impacted capacities estimated by probabilistic over deterministic approaches. Using **Table 6**, the new factor, ψ, can be estimated through Equation (28).

$$\psi = \frac{\zeta_P}{\zeta_D} \tag{28}$$

where: ψ represents the safety factor, and ζ_P and ζ_D are the factors utilized to determine specific low velocity post vehicle impacted residual capacities estimated by using probabilistic and deterministic approaches respectively.

Using Equation (28), ζ is normalized to obtain a coherent relationship between respective factors and percent damage to determine the distress level as shown in **Figure 11**.
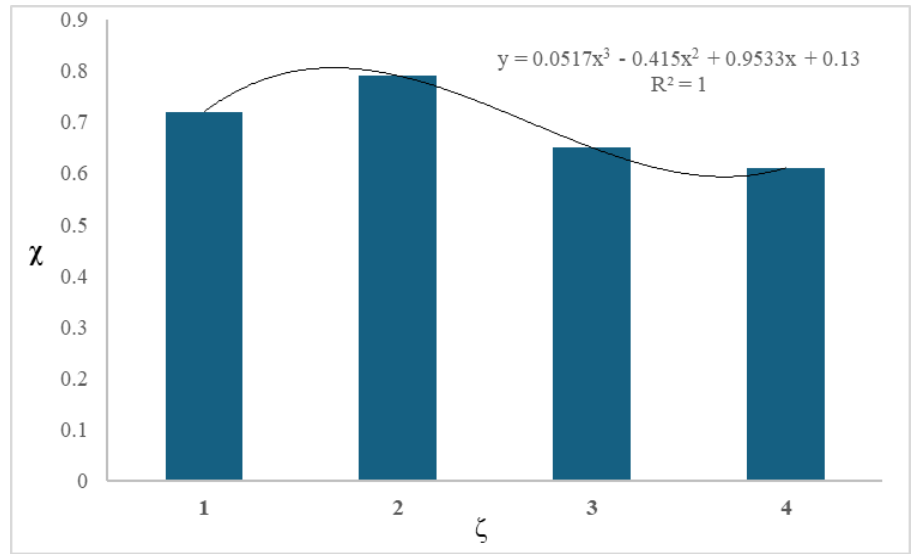
Figure 11. χ and ζ.

From **Figure 11** a significant relationship between χ and ζ shall be obtained by using a polynomial equation with a tight R^2 value of 1, as shown in Equation (29).

$$\chi = 0.052\zeta^3 - 0.415\zeta^2 + 0.953\zeta + 0.13 \tag{29}$$

where: χ represents percent damage level and ζ specifies low velocity post vehicle impacted residual capacity incurred from individual impact scenario.

To precisely predict the uncertainty (Π) parameter, partial derivative of using the test results (R) and utilizing independent variables (x_i where i = 1, 2, 3, …, n) and individual uncertainties (Π_i where i = 1, 2, 3, …, n) can be employed as shown in Equation (30) [39].

$$\Pi = \pm \left[\left\{ \frac{\partial R}{\partial x_1} \Pi_1 \right\}^2 + \left\{ \frac{\partial R}{\partial x_2} \Pi_2 \right\}^2 + \cdots + \left\{ \frac{\partial R}{\partial x_n} \Pi_n \right\}^2 \right]^{1/2} \tag{30}$$

After reducing multiple variables into two variables, i.e., χ and ζ being dependent and an independent variable, Equation 30 has been normalized to the two parameters in determining the uncertainty parameter (Π). For individual uncertainty in finding ζ, mean value, i.e., ζ_m has been utilized conservatively. However, simplification in estimating uncertainty (Π) using Equation (30) can be determined by using a total derivative as shown in Equation (31) [35].

$$\Pi = \pm \left[\frac{d(\chi)}{d(\zeta)} \right] \times \{\zeta_m\} \tag{31}$$

where: Π, χ, ζ, and ζ_m have already been addressed.

Equation (31) yields Π as ± 0.31 or $\pm 31\%$. However, Π predominately depends on a single variable parameter (ζ), and hence seems to be highly optimistic and a little conservative as well.

7. Conclusions and future works

This research instills an insight to quantify the severity of damage to the impacted RC piers exposed to low to cosmetic vehicle collision. This study examines the damage incurred by the low velocity impact and investigate the shear and axial capacities of the representative circular RC bridge pier as concrete is exposed to

vehicle collisions. To make it, deterministic analysis by incorporating damage index (DI) is utilized to determine the P_f and corresponding residual capacities. To capture the uncertainties included, the strength of the post impacted test piers conforming similar geometries are further scrutinized through resistance reduction method (RRM) via reliability analyses, and utilizing it through the LSE, the P_f of the impacted pier at specific dynamic load has been determined. The λ and RRM are then used as a multiplier determining the L_R to obtain the reduced design capacities.

A new factor (μ) has been introduced to correlate between reduced resistance estimated by probabilistic and deterministic methods. The difference in determining the post damaged capacity estimated by probabilistic method provides 8.68% increase than deterministic analyses for sub-compact collision, whereas presents a conservative result of 6.86% for being damage incurred by mid-size sedan car incorporating both axial and shear capacities as shown in **Table 6**.

This study will help develop the correlations between deterministic and probabilistic approaches and vice versa and can serve as an important tool for practitioners.

- Experimental studies executed on the representative pier's specimens, and the corresponding equivalent impact data are converted into realistic low velocity car impacts with RC pier data. Reliability studies are carried out to apprehend the post impacted pier performance for capturing reduced capacity via using P_f.

- Deterministic method using DI approach provides better and optimistic results in evaluating L_R for low vehicle impact damage incurred by sub-compact car compared to the mid-size sedan car.

- Probabilistic analyses using RRM provides precise results for estimating the cosmetic damage experienced by mid-size sedan car capturing all uncertainties involved in deterministic approach.

- The results are summed up by introducing a safety factor (μ) via parametric study to precisely capturing the low to cosmetic impact damage.

- A representative relationship between χ and ζ can precisely help to capture percent damage level along with post impacted residual capacity of the low velocity impact.

- The uncertainty parameter, Π, being ± 0.31 ($\pm 31\%$) seems to be a little conservative as the variables (x_i) are normalized to a single parameter, ζ. This normalization using ζ_m helps analyzing the intrinsic uncertainties hidden in capturing low velocity impact damage.

- However, future work must include a substantial number of experimental studies to be carried out at medium to higher velocity impact at high strain rate load and at different collision scenarios, involve various geometries, and utilize different material properties prior to applying the results for extensive use.

Conflict of interest: The author declares no conflicts of interest.

Abbreviations

Symbols

f_{cd}	Dynamic compressive strength at the dynamic strain rate
$\acute{\varepsilon}_d$	Dynamic strain rate of concrete
f_{cs}	Static compressive strength as quasi-static strain rate
$\acute{\varepsilon}$	Quasi-static strain rate at concrete
DIF	Dynamic increase factor
CDIF	Dynamic increase factor for concrete in a compression
α	Dynamic constant
f_{cu}	Cube compressive strength
M	Weight of semi-trailer vehicle
V	Impact velocity
F_{max}	Frontal impact force
t	Duration of impact
E	Total impact energy
I_r	Frontal shock (force) due to vehicle impact
$I_{r,max}$	Frontal overpressure
t_d^+	Positive phase for impact pressure
γ	Decay co-efficient of the waveform
I_{dyn}	Dynamic impact force
λ	Damage index
f_c'	28 days' compressive strength of concrete
σ_o	Yield strength of steel
A_g	Gross cross-sectional area of concrete
A_s	Total cross-sectional area of longitudinal steel
h_I	Height of fall for impact
p	Transverse steel ratio
V_c	Shear strength carried by concrete
V_s	Transversal shear capacity
v_b	Shear constant
A_h	Area of single hoop for transverse steel
ρ_t	Longitudinal steel ratio
D	Spiral diameter of transversal steel
σ_{yh}	Yield stress of transverse steel
d_b	Bar diameter
$P_{N,design}$	Axial capacity of pier
$V_{N,design}$	Shear capacity of pier
L_{Design}	Design axial or shear load carrying undamaged reinforced concrete bridge pier
$L_{Residual}$	Residual strength for axial or shear of the damaged pier
f_y	Static yield strength of steel
P_f	Probability of failure
β	Reliability index

Φ	Reliability function
Φ^{-1}	Inverse of the tail probability function
E_c	Elastic modulus of concrete
$f'_{c,d}$	Dynamic compressive stress of concrete
ζ	Residual capacity
ζ_P	Factor used to determine residual capacities using probabilistic approach
ζ_D	Factor used to determine residual capacities using deterministic analyses
χ	Percent damage level
ψ	Safety factor
Π	Uncertainty parameter
R	Test result
x_i	Independent variables
Π_i	Individual uncertainties of variable

Conversion chart for the US customary to the equivalent SI units

US Customary	SI Unit
1 ksi	6.89 MPa (kN/mm^2)
1 psi	0.00689 Mpa (kN/mm^2)
1 kip-in	0.113 kN-m
1 kip	4.45 kN
1 lbs	0.00445 kN
1 mph	1.61 km/hr
1 ft-lb/sec	0.00136 kN-m/sec (1.36 N-m/sec)
1 in	0.0254 m (25.4 mm)

References

1. Cook W. Bridge Failure Rates, Consequences, and Predictive Trends [PhD thesis]. Utah State University. 2014; p. 116.
2. Wiacek C, Nagabhushana V, Rockwell T, et al. Evaluation of frontal crash stiffness measures from the US New car assessment program. In: Proceedings of the ESV Conference; 2015; Seoul, South Korea.
3. Der Kiureghian A. Analysis of structural reliability under parameter uncertainties. Probabilistic Engineering Mechanics. 2008; 23(4): 351–358.
4. Malvar LJ, Crawford JE. Dynamic increase factors for concrete. In: Proceedings of the 28th DDESB Seminar; September 1998; Orlando.
5. Sharma H, Hurlebaus S, Gardoni P. Performance-based response evaluation of reinforced concrete columns subject to vehicle impact. International Journal of Impact Engineering. 2012; 43: 52-62. doi: 10.1016/j.ijimpeng.2011.11.007
6. Auyeung S, Alipour A, Saini D. Performance-based design of bridge piers under vehicle collision. Engineering Structures, Elsevier. 2019; 191: 752–765.
7. Zhou D, Li R. Damage assessment of bridge piers subjected to vehicle collision. Advances in Structural Engineering. 2018a; 21(15), 2270–2281.
8. Buth CE, Brackin MS, Williams WF, Fry GT. Collision Loads on Bridge Piers: Phase 2. Report of Guidelines for Designing Bridge Piers and Abutments for Vehicle Collisions. 2011.
9. Alipour A, Shafei B, Shinozuka M. Reliability-Based Calibration of Load and Resistance Factors for Design of RC Bridges under Multiple Extreme Events: Scour and Earthquake. Journal of Bridge Engineering. 2012; 18(5).
10. Engineers AS. Minimum Design Loads for Buildings and Other Structures (ASCE/SEI 7-10). American Society of Civil Engineers; 2013.
11. Mander JB., Priestley MJ, Park R. Theoretical stress-strain model for confined concrete. Journal of Structural Engineering

(United States). 1988; 114(8): 1804–1826.

12. Malvar LJ, Crawford JE. Dynamic increase factors for steel reinforcing bars. In: Proceedings of the 28th DDESB Seminar; 1998; Orlando, USA.

13. Roy S, Sorensen A. A Reliability Based Crack Propagation Model for Reinforced Concrete Bridge Piers Subject to Vehicle Impact. In: Proceedings of the 18th International Probabilistic Workshop: IPW 2020.

14. Ameli MJ, Pantelides CP. Seismic analysis of precast concrete bridge columns connected with grouted splice sleeve connectors. Journal of Structural Engineering, American Society of Civil Engineers. 2017; 143(2): 4016176.

15. Federal Highway Administration. Concrete Bridge Shear Load Rating Synthesis Report. Available online: https://www.fhwa.dot.gov/bridge/loadrating/pubs/hif18061.pdf (accessed on 12 May 2024).

16. ACI. ACI 318-11: Building Code Requirements for Structural Concrete. American Concrete Institute; 2011.

17. ACI committee 318. Building code requirements for structural plain concrete (ACI 318.1-83) and commentary. International Journal of Cement Composites and Lightweight Concrete. 1985; 7(1); 60.

18. AFDC. Vehicle Weight Classes & Categories. Alternative Fuels Data Centre, U.S. Department of Energy; 2018.

19. Birely AC, Yole KJ, Lee JD, et al. Experimental behavior of reinforced concrete and pretensioned concrete bent caps. Journal of Bridge Engineering, American Society of Civil Engineers. 2020; 25(2): 4019137.

20. Thomas RJ, Steel K, Sorensen AD. Reliability analysis of circular reinforced concrete columns subject to sequential vehicular impact and blast loading. Engineering Structures. 2018; 168: 838-851. doi: 10.1016/j.engstruct.2018.04.099

21. Vrouwenvelder T. Stochastic modelling of extreme action events in structural engineering. Probabilistic Engineering Mechanics. 2000; 15(1): 109–117.

22. Zhou D, Li R, Wang J, Guo C. Study on Impact Behavior and Impact Force of Bridge Pier Subjected to Vehicle Collision. Shock and Vibration. 2017; 1–12.

23. Roy S, Unobe I, Sorensen AD. Vehicle-Impact Damage of Reinforced Concrete Bridge Piers: S State-of-the Art Review. J. Perform. Constr. Facil., American Society of Civil Engineers. 2021; 35(5): 03121001.

24. Roy S, Unobe ID, Sorensen AD. Reliability assessment and sensitivity analysis of vehicle impacted reinforced concrete circular bridge piers. Structures, Elsevier. 2022; 37: 600–612.

25. Roy S, Sorensen A. Energy Based Model of Vehicle Impacted Reinforced Bridge Piers Accounting for Concrete Contribution to Resilience. In: Proceedings of the 18th International Probabilistic Workshop: IPW 2020. p. 301.

26. Roy S. Sustainability and Resiliency Investigation of Grouted Coupler Embedded in RC ABC Bridge Pier at Vehicle Impact, Engineering and Applied Sciences. 9(2024): 14–33. doi: https://doi.org/10.11648/j.eas.20240901.12

27. AASHTO. Guide Specifications for LRFD Seismic Bridge Design, 2nd ed. American Association of State Highway and Transportation Officials; 2011.

28. AASHTO M145-91. American Association of State Highway and Transportation Officials. Classification of Soils and Soil-Aggregate Mixtures for Highway Construction Purposes. American Association of State Highway and Transportation Officials; 2008. p. 9.

29. Cowper G, Symonds P. Strain hardening and strain-rate effects in the impact loading of cantilever beam. Brown University Division of Applied Mathematics; 1957. pp. 1–46.

30. Feyerabend M. Hard transverse impacts on steel beams and reinforced concrete beams. University of Karlsruhe (TH), Germany; 1988.

31. Shi Y, Hao H, Li ZX. Numerical derivation of pressure-impulse diagrams for prediction of RC column damage to blast loads. International Journal of Impact Engineering. 2008; 35(11): 1213-1227. doi: 10.1016/j.ijimpeng.2007.09.001

32. Ayyub BM, McCuen RH. Probability, statistics, and reliability for engineers and scientists. CRC press; 2016.

33. Bathurst RJ, Allen TM, Nowak AS. Calibration concepts for load and resistance factor design (LRFD) of reinforced soil walls. Canadian Geotechnical Journal. 2008; 45(10): 1377–1392.

34. Nowak AS, Collins KR. Reliability of Structures. CRC Press; 2012. doi: 10.1201/b12913

35. Dietenberger M, Buyuk M, Kan CD. Development of a High Strain-Rate Dependent Vehicle Model. LS-DYNA Anwenderforum. 2005.

36. Schultz GG, Seegmiller L. Utah Commercial Motor Vehicle Weigh-in-Motion Data Analysis and Calibration Methodology. Engineering, Environmental Science. 2006.

37. Joshi AS, Gupta LM. A simulation study on quantifying damage in bridge piers subjected to vehicle collisions. International Journal of Advanced Structural Engineering. SpringerOpen. 2012; 4(1).

38. Mestrovic D, Cizmar D, Miculinic L. Reliability of concrete columns under vehicle impact. In: WIT Transactions on the Built Environment. WIT Press; 2008. doi: 10.2495/su080161

39. Holman JP. Experimental methods for engineers, 6th ed. McGraw-Hill; 1994.